Research Report

Development of Wettability Evaluation Technique Applying Contact Angle Measurement during Soldering

Hisaaki Takao, Toshihiko Tsukada, Keiichi Yamada,
Masahiko Yamashita, Hideo Hasegawa

Abstract

A new wettability evaluating system was developed by combining a contact angle measurement instrument, which optically and in-situ measures the contact angle of molten solder, with a conventional wettability tester (meniscograph). Using this new evaluation system, a well-known experiential knowledge that the wettability for Sn-3.5Ag, a typical Pb-free solder, is inferior to that for Sn-37Pb is quantitatively confirmed by the result that the contact angle for Sn-3.5Ag is twice of that for Sn-37Pb. The cause for this wettability difference is attributed to the difference in the surface tensions of the solders (the solder-flux interfacial tension). The influences of alloying elements (1%Cu, 1%Zn, 5%Bi, 5%In), fluxes and Au coating on a Cu substrate on the wettability for the Sn-3.5Ag are discussed. In the discussion, three interfacial tensions among the solder, flux and substrate are separately estimated to analyze the mechanisms which make differences in wettability.

Keywords Solder, Contact angle, Interfacial tension, Wettability, Meniscograph method

1. Introduction

Wettability is an essential characteristic of a soldering system for electronics. To quantitatively evaluate the wettability, the contact angle and interfacial tension should be first measured. There have been only a few reports, however, on wettability of practical soldering systems because of the difficulty to measure these physical parameters in the presence of flux.

A meniscograph method (wetting balance method)[1] is one of the most commonly used wettability evaluation methods. In this method, a force on a substrate, while the substrate is immersed in a molten solder bath and is wetted by the solder, is measured. Indices of wettability, such as wetting time and wetting force, can be evaluated by the analysis of obtained force-time curves (wetting curve). The measured indices of wettability, however, are easily affected by the substrate size and shape because the wetting curve depends on the heat capacity.[2] Consequently, the measured wettability is not quantitative, but only qualitative.

In addition, this method can measure neither the contact angle (θ) nor interfacial tension (γ_{lf}) directly, which are essential physical parameters of wetting. Some methods have been proposed, however, to separately estimate them, utilizing the fact that the wetting force is the product of these two parameters.[3] Vianco[4] estimated the contact angle and interfacial tension by a theoretical analysis of the wetting height and wetting force of a solder. Vincent and Humpston[5] and Miyazaki et al.[6] each proposed a method measuring γ_{lf} by using the substrate which is not wetted by molten solder, e.g., Teflon or Al_2O_3.

In this study, we developed a new wettability evaluation system, which is obtained by combining an instrument to directly measure the contact angle (θ) during the solder wetting process with a conventional wettability tester (meniscograph tester). In addition to the wettability indices measured by the meniscograph tester, the contact angle (θ) and interfacial tension (γ) can be simultaneously measured with this system. In this report, this newly developed system is described and some applications to the evaluation and analysis of the wettability are presented.[7, 8]

2. Wettability evaluation system using the contact angle measuring instrument

Figure 1 shows a vertical schematic illustration of a substrate immersed in molten solder. The wetting force (F) is related to the contact angle (θ) and solder-flux interfacial tension (γ_{lf})[3] as:

$$F = P \cdot \gamma_{lf} \cdot \cos\theta - B \quad \ldots\ldots\ldots\ldots\ldots\ldots (1)$$

where P is the perimeter of the substrate, and B is the buoyancy force, both of which are known to be constants. When F and θ are measured, γ_{lf} can be obtained from Eq. (1). In this study, the contact angle and wetting force (F) measured 5s after immersion were used.

Figure 2 is a schematic illustration of wetting. The contact angle is determined by the balance of three interfacial tensions at the wetting tip of the solder, i.e., solder-flux (γ_{lf}), substrate-flux (γ_{sf}) and substrate-solder (γ_{sl}) interfacial tensions. This relationship[9] is described by Young's Eq. (2).

$$\gamma_{sf} = \gamma_{lf} \cdot \cos\theta + \gamma_{sf} \quad \ldots\ldots\ldots\ldots\ldots\ldots (2)$$

Using Eqs.(1) and (2), the difference: $\gamma_{sf} - \gamma_{sl}$ can be

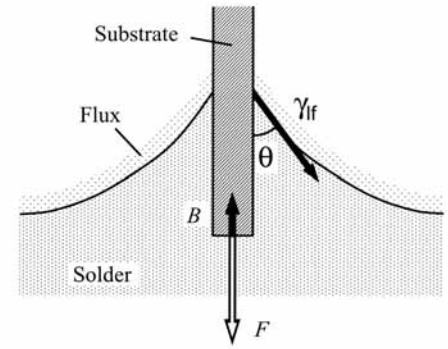

Fig. 1 Vertical schematic illustration of the substrate immersed in the molten solder using the meniscograph method.

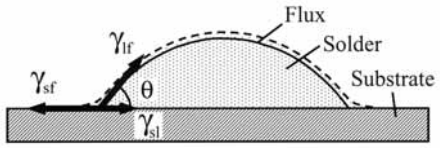

Fig. 2 Sessile drop geometry determined by the equilibrium relationship between the solder-flux, substrate-flux, and substrate-solder interfacial tension.

obtained.

To measure a contact angle, a three-dimensional profile of the molten solder fillet must be determined quickly and accurately because wetting of molten solder on a substrate completes within a few seconds. Conventional methods,[10-13] however, do not have enough speed and accuracy.

Figure 3 shows the construction of the contact angle and interfacial tension measuring system with a meniscograph instrument. The contact angle measurement is based on the regular reflection on a molten solder surface, which possesses a specular gloss. The following techniques were employed to achieve a high speed (15 frame/s) and highly accurate ($\pm 0.2^{o}$) measurement.

(1) To improve the angular resolution of this instrument, multiple light sources (37 LEDs) are accurately arranged at an interval of 2.2^{o} as shown in **Fig. 4**. The wavelength of the LEDs were selected to be 880nm (near-infrared light) to suppress the influence of visible light.

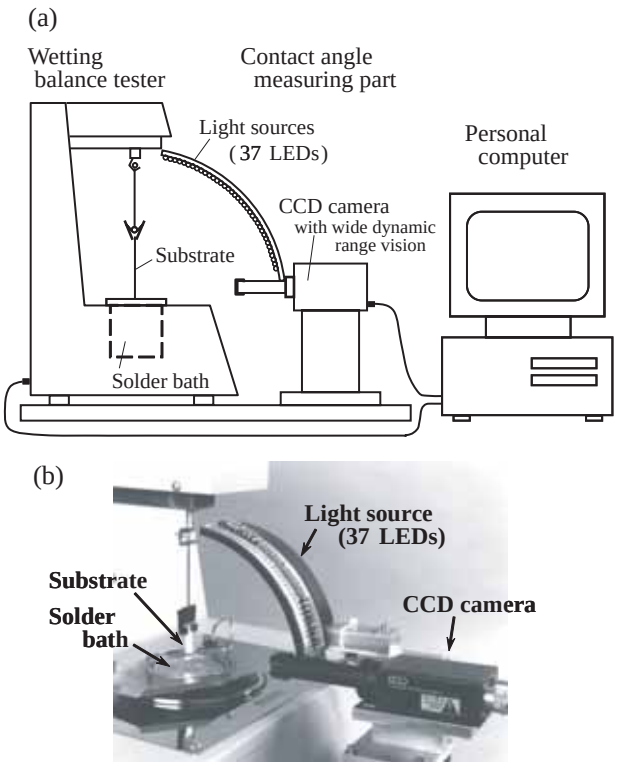

Fig. 3 Wettability evaluation system using the conventional meniscograph tester combined with the contact angle measuring instrument: (a) construction of the system, and (b) contact angle measuring part.

(2) To accurately specify the position of the light source, two different lighting patterns: patterns A and B were used, as shown in **Fig. 5**, and each LED was uniquely coded by the ratio of brightnesses between the two patterns. Detail of this technique is as follows. All LEDs, whose brightnesses are accurately controlled by resistors, and simultaneously irradiate the molten solder surface. In lighting pattern A, the brightnesses of the light sources are set in the decreasing order from 1 to 37.

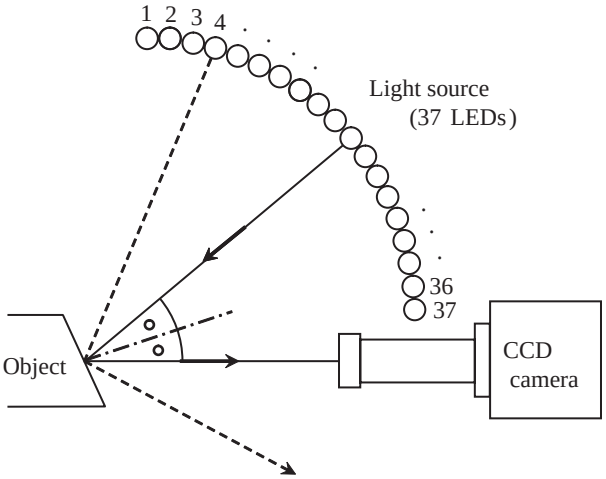

Fig. 4 Principle of specular surface orientation detection using regular reflection light.

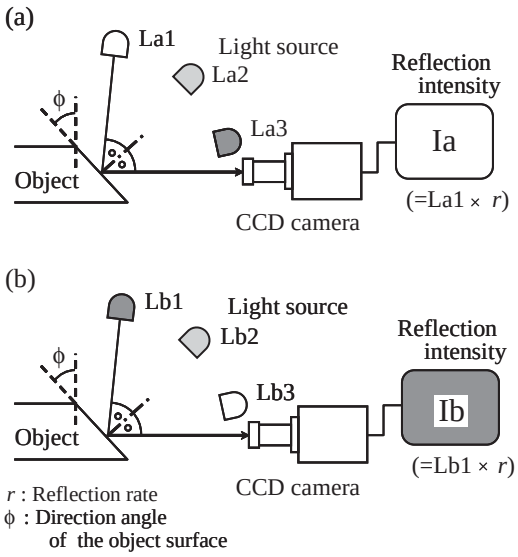

Fig. 5 Schematic illustration of the brightness-ratio-coded method; (a) lighting pattern A (brightness: La1>La2>La3), and (b) lighting pattern B (brightness: Lb1<Lb2<Lb3).

In contrast, in lighting pattern B, the brightnesses of the light sources are set in the increasing order from 1 to 37. It should be noted that the ratio of brightnesses between the two patterns is unique for each LED. The reflected light is recorded with a CCD camera as a light spot. The intensity ratio of each reflected light spot is equal to that of light source as:

$$Ia / Ib = (Lal \cdot r) / (Lb1 \cdot r) = La1/Lb1 \quad \ldots\ldots (3)$$

where Ia and Ib are the reflection intensities on a reflected light spot for pattern A and pattern B, respectively, La1 and Lb1 are the respective brightnesses of the light source, and r is the reflection ratio of the solder surface. Therefore, without knowing r, one can tell the brightness ratio of the light source by evaluating the ratio of the reflection intensity, i.e., which one of 37 LEDs is the light source of the measured light spot. Then, because the surface reflection is regular, the direction angle (ϕ) of the solder fillet surface is determined.

(3) The dynamic range of the CCD camera was enlarged by synthesizing two pictures obtained under two different exposure periods of time[14] to enlarge the recordable brightness range and therefore to enable more accurate measurement.

(4) **Figure 6** shows the sequence of the lighting patterns and two exposure periods. In this sequence, four images are taken: two exposure periods for each of two lighting patterns. To avoid the change of the solder fillet shape during wetting, the recording time-lags among the four images were minimized by the control of the exposure time by changing the irradiation period of time of LEDs and synchronizing it with the field of the CCD camera.

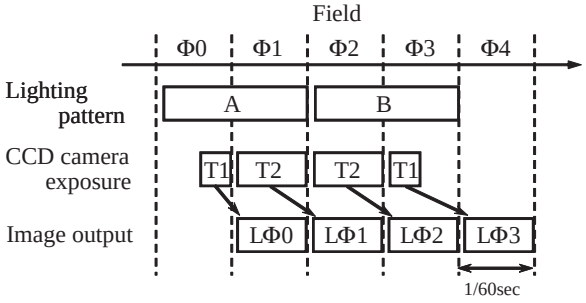

Fig. 6 Timing chart of imaging.

3. Wettability evaluation using the developed system

3. 1 Performance of the wettability evaluation system

The contact angle measuring instrument is shown in **Table 1**. **Figures 7** show the result of the wettability measurement of the 63mass%Sn-37mass%Pb eutectic solder (hereinafter Sn-37Pb) using a Cu plate ($10\times30\times0.3$ (mm^3)) as the substrate and a halogen-free RMA type flux at the soldering temperature of 230°C. Before the wettability test, the Cu plate surface was cleaned by electrolytic polishing, followed by etching with 1M HCl, washing in ion-exchange water and then drying in the air.

Figures 7(a) and (b) show a 3-D solder fillet

Table 1 Performance of contact angle measuring instrument.

Sampling area (mm^2)	3.16(X) × 2.45(Y)
Resolution (pixel)	640(H) × 240(V)
Measured angle range*1 (deg)	(1)4-42, (2)18-56, (3)33-71
Accuracy of angle*2 (deg)	±0.2
Sampling rate (frames max./sec)	15

*1: It can be selected on the setting angle of CCD camera for horizontal level.
*2: Maximum fluctuation on one pixel is ±2deg.

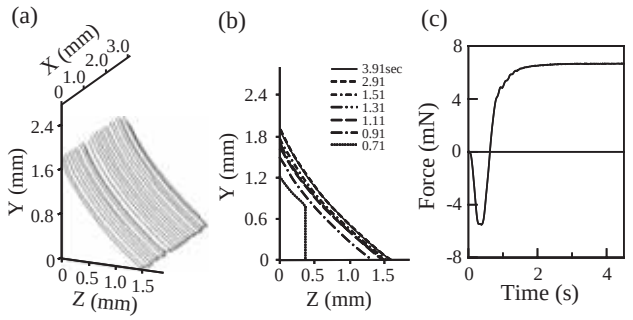

Fig. 7 Measurement example of Sn-37Pb solder wetting on Cu substrate at 230°C: (a) 3D-solder fillet profile, (b) its time-changes, and (c) wetting curve measured by conventional meniscograph method. In Fig. 6(b), there is no data for the fillet profile at 0.71s in the Z value beyond 0.35mm because the direction angles of the solder fillet surface were beyond the measurable angle.

profile and the change over time of the cross-sectional view. Figure 7(c) is a wetting curve from the meniscograph test. The solder fillet profiles shown in Figs. 7(a) and (b) were obtained by integrating the obtained angle data from the tip of the solder to the bottom. In Fig. 7(b), there is little change in the cross-sectional solder fillet profiles after 2.91s from the immersion. This agrees with the wetting curve in Fig. 7(c), which has little change after that time also. This result exhibits the ability of this system well.

Another examination was conducted to clarify the influence of the shape of the substrate on the wettability, which is easily influenced in the conventional meniscograph method. In this experiment, a Cu plate (10mm in width, 30mm in length and 0.3mm in thickness) and a Cu wire (a diameter of 1.2mm and length of 30mm) were compared under the same experimental conditions as described before except for the solder (96.5mass%Sn-3.5mass%Ag eutectic solder (hereinafter Sn-3.5Ag)) and the soldering temperature (270°C). The measured results are shown in **Table 2**. The values of θ and γ_{lf} for both substrates agree well. This result shows that the measurement by this system is not influenced by shapes of the substrate.

3. 2 Application to solder wettability evaluation and analysis

Using this newly developed system, we compared the wettability for Sn-3.5Ag with that for Sn-37Pb, and moreover, investigated the influence of the alloying elements (Cu, Zn, In, Bi) of Sn-3.5Ag, fluxes and a coating on a substrate. **Table 3** shows the conditions of the wettability test. As the substrate, Cu (10×30×0.3mm^3) and Au-coated (70nm thickness by sputtering) Cu (described as Au/Cu hereafter) plates were used. Before the wettability test and coating with the noble metal, the Cu plate surface was cleaned in the same manner as described before. In the investigation of the influence of fluxes, the same RMA type flux as described before and a more activated flux were used. The soldering temperature was measured at a depth of 3mm from the surface of the molten solder with a thermocouple.

3. 2. 1 Comparison of wettabilities for Sn-3.5Ag and Sn-37Pb

Figure 8 shows the θ values between Sn-3.5Ag or Sn-37Pb and the Cu substrate. The θ values for Sn-

Table 2 Contact angle and flux-solder interfacial tension on the Cu substrates wetted by Sn-3.5Ag solder at 270°C.

	Substrate	
	Cu plate	Cu wire
θ(deg)	42.5 (42.2-42.9)	42.7 (41.4-44.5)
γ_{lf} (N/m)	0.470 (0.462-0.477)	0.505 (0.486-0.511)

upper : average and lower: distribution of measurements

Table 3 Experimental conditions of wettability test.

Solder alloy	Sn-3.5Ag, Sn-3.5Ag-1.0Cu, Sn-3.5Ag-1.0Zn, Sn-3.5Ag-5.0In, Sn-3.5Ag-5.0Bi, Sn-37Pb
Temperature	230, 250, 270, 290°C
Substrate	Cu, Au/Cu
Flux	PO-Z-7(Senzyu), ULF-300R(Tamura)
Atmosphere	air
Immersion time	10 s
Immersion depth	10 mm
Immersion rate	10 mm/s
Repetition	3

Au/Cu: Au (70nm) coated Cu substrate

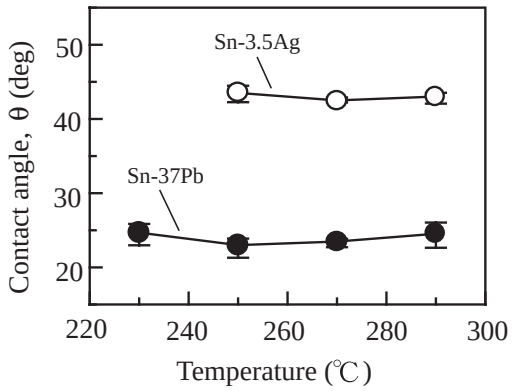

Fig. 8 Contact angle of Sn-3.5Ag and Sn-37Pb wetting on Cu substrate. There are no data for Sn-3.5Ag at 230°C because the wetting was too unstable to measure the θ value.

3.5Ag are twice of those for Sn-37Pb and hence, the wettability for Sn-3.5Ag is significantly inferior to that for Sn-37Pb.

Table 4 shows θ, γ_{lf} and γ_{sf} - γ_{sl} for the wetting between Sn-3.5Ag or Sn-37Pb and the Cu substrate at 270°C γ_{lf} for Sn-3.5Ag is larger than that for Sn-37Pb, while γ_{sf} - γ_{sl} for Sn-3.5Ag is almost equal to that for Sn-37Pb. According to Young's equation shown in Eq. (3), this means that the low wettability for Sn-3.5Ag is due to the larger γ_{lf}.

3. 2. 2 Influence of alloying element in Sn-3.5Ag on wettability between solder and substrate

Table 5 shows θ and γ for the wetting between Sn-3.5Ag-X (X = Cu, Zn, In and Bi) and the Cu substrate at 270°C. Contact angle is in the increasing order of Sn-3.5Ag-5Bi (θ = 38°), Sn-3.5Ag-5In (θ = 41°), Sn-3.5Ag-1Cu (θ = 42°), Sn-3.5Ag (θ = 43°), Sn-3.5Ag-1Zn (θ = 48°). Although the wettability for the Sn-3.5Ag alloy is only slightly influenced by the addition of Cu or In, the wettability is improved by the addition of Bi, and decreased by the addition of Zn. From the comparison of γ, these differences in the wettability are again attributed to the difference in γ_{lf}, not that in γ_{sf} - γ_{sl}.

3. 2. 3 Influence of fluxes on wettability between Sn-3.5Ag and Cu substrate

Table 6 shows the influence of fluxes on θ and γ for the wetting between Sn-3.5Ag and the Cu substrate at 270°C. Using a more activated flux (ULF-300R) containing halogen rather than a flux without a halogen (PO-Z-7) decreases θ, i.e., improves the wettability. From the comparison of γ, this wettability improvement is due to the decrease in γ_{lf}.

3. 2. 4 Influence of Au coating on Cu substrate on wettability for Sn-3.5Ag

Table 7 shows θ and γ for the Cu substrate and the Au/Cu substrate wetted by Sn-3.5Ag at 270°C. The contact angle decreases from 43° to 29° by coating the Cu substrate with Au and hence, the wettability of the substrate is remarkably improved. The improvement in the wettability is attributed to the increase in γ_{sf} - γ_{sl}. It should be noted that θ between Sn-3.5Ag and the Au/Cu substrate is equivalent to that for Sn-37Pb on the bare Cu substrate (θ = 23° shown in Table 4). The substrate-flux interfacial tension (γ_{sf}) is considered to be influenced by the noble metal surface on Cu substrate. However, this is not necessarily true for the substrate-solder interfacial tension (γ_{sl}) because Au coating of 70nm

Table 4 Contact angle and interfacial tension on Cu substrate wetted by Sn-3.5Ag and Sn-37Pb at 270°C.

Solder	θ(deg)	γ_{lf} (N/m)	γ_{sf} - γ_{lf} (N/m)
Sn-3.5Ag	43	0.470	0.347
Sn-37Pb	23	0.385	0.353

Table 5 Influence of added element to Sn-3.5Ag on contact angle and interfacial tension on Cu substrate at 270°C.

Solder	θ(deg)	γ_{lf} (N/m)	γ_{sf} - γ_{sl} (N/m)
Sn-3.5Ag	43	0.470	0.347
Sn-3.5Ag-1.0Cu	42	0.462	0.346
Sn-3.5Ag-1.0Zn	48	0.508	0.338
Sn-3.5Ag-5.0In	41	0.456	0.345
Sn-3.5Ag-5.0Bi	38	0.423	0.335

Table 6 Influence of flux on contact angle and interfacial tension on Cu substrate wetted by Sn-3.5Ag at 270°C.

Flux	θ(deg)	γ_{lf}(N/m)	γ_{sf} - γ_{sl}(N/m)
PO-Z-7	43	0.470	0.347
ULF-300R	38	0.406	0.320

(PO-Z-7 : without halogen and ULF-300R: with halogen)

Table 7 Influence of the surface coating on Cu substrate on contact angle and interfacial tension of Sn-3.5Ag at 270°C.

Coating/Substrate	θ(deg)	γ_{lf}(N/m)	γ_{sf} - γ_{sl}(N/m)
--- / Cu	43	0.470	0.347
Au / Cu	29	0.460	0.402

(Thickness of Au coating layer : 70 nm)

thickness might be too thin to sustain when it is wetted with a solder.

X-ray diffraction analysis showed that Cu_6Sn_5 is formed at both the solder/substrate interfaces, which was the same intermetallic compound as the one found in previous studies.[15, 16] It appears that the 70nm-Au coating layer dissolves into the molten solder, and the solder reacts with the Cu substrate directly. Because γ_{sl} acts between a solder and the intermetallic compound, γ_{sl} on the Au/Cu substrate is likely the same with that on the bare Cu substrate.

Therefore, the difference in γ_{sf} - γ_{sl} between the Au/Cu substrate and the Cu substrate is considered to result from the difference in γ_{sf}. The decrease in θ and hence, the wettability improvement by coating the Cu surface with Au is attributed to the increase in γ_{sf}.

3. 2. 5 Relationship between contact angle and spreading factor

The spreading factor is another index of wettability, which is easier to measure than θ, and therefore, commonly used. A Japanese Industrial Standard (JIS) defines its measurement in which it is measured from the heights of a solder before and after it is spread on a substrate.[17]

Figure 9 shows the measured correlation between θ and the spreading factor for the various solders with a calculated line which is derived from the assumption[18] that a solder spread on a substrate forms a spherical surface. The experimental correlation indicates that wettability can be estimated relatively by measuring the spreading factor. Absolute values of θ predicted from measured spreading factors using the theoretical curve, however, are much smaller than actual values. This suggests that the spherical surface assumption is invalid probably because the top of droplet is depressed by gravity.

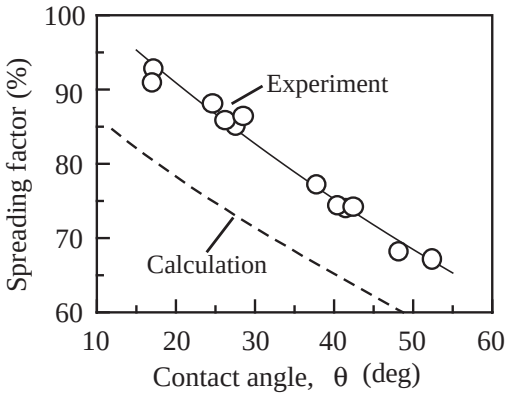

Fig. 9 Relationship between contact angle measured by this system and spreading factor measured by spreading test.

4. Summary

We have developed a new wettability evaluation system. The following conclusions were derived from the present study.

(1) With the newly developed wettability evaluation system, the contact angle (θ) and interfacial tension (γ) can be directly measured.

(2) Using the relationship among the wetting force, θ and γ, the solder-flux interfacial tension (γ_{lf}) and the difference between the substrate-flux interfacial tension (γ_{sf}) and substrate-solder one (γ_{sl}) can be obtained. Therefore, the wettability can be analyzed from the viewpoint of the interfacial tensions.

(3) γ_{lf} value of Sn-3.5Ag is larger than that of Sn-37Pb. This is the reason why θ for the wetting for Sn-3.5Ag is much larger than that for Sn-37Pb.

(4) The wettability between Sn-3.5Ag alloys and a Cu substrate is in the decreasing order of Sn-3.5Ag-5Bi, Sn-3.5Ag-5In, Sn-3.5Ag-1Cu, Sn-3.5Ag, Sn-3.5Ag-1Zn. This difference is attributed to the difference in γ_{lf}.

(5) Using a more activated flux containing halogen rather than one without halogen, the wettability between Sn-3.5Ag and a Cu substrate is improved. This improvement is attributed to smaller γ_{lf} with the flux containing halogen.

(6) Au coating of 70 nm thickness on the Cu substrate drastically improves the wettability between Sn-3.5Ag and a Cu substrate. This improvement is attributed to the increase in γ_{sf} rather than the decrease in γ_{sl}.

This wettability evaluation system possesses all the requirements for JIS Z 3198-4 (Test methods for lead-free solders -- Part 4: Methods for solderability test by a wetting balance method and a contact angle method). We expect that it will be used as a standard measuring method for quantitatively

evaluating the wettability for various Sn-Pb or Pb-free solder alloys, substrates and fluxes.

Acknowledgments

This research was supported by Mr. K. Nonaka Y. Suzuki and M. Matsui at Toyota Central R&D Labs., Inc. for technical support of developing the contact angle measuring instrument. Dr. Yu Morimoto is also acknowledged for critically reviewing the manuscript.

References

1) Japanese Standards Association: JIS C 0053, (1996) Japanese Standards Association, Tokyo
2) Okamoto, I., Takemoto, T., Mizutani, M. and Mori, I. : Trans. JWRI, **14**(1985), 21-27
3) Takemoto, T. and Sato, R. : *Kousinraido Maikurosorudaringu Gijutu*, (in Japanese), (1991), 84, Kogyo Chosakai Publishing Co., LTD., Tokyo
4) Vianco, P. T. : The Metal Science of Joining, (1992), 265-284, The Minerals, Metals & Materials Society
5) Vincent, J. H. and Humpston, G. : GEC J. Res., **11**(1994), 76-89
6) Miyazaki, M., Mizutani, M., Takemoto T. and Matsuawa, A. : J. Japan Welding Soc., **115**(1997), 681-687
7) Yamada, K. and Yamamoto, S. : Trans. IEE Jpn., **116**-C(1996), 898-904
8) Takao, H., Tsukada, T,. Yamada, K., Yamashita, M. and Hasegawa, H. : J. Jpn. Inst. Electron. Pack., **6**(2003), 488-495
9) Young, T. : Trans. Roy. Soc., **95**(1805), 65-87
10) Sanderson, A. C., Weiss, L. E. and Nayar, S. K. : IEEE Trans. Pattern Anal. & Mach. Intell., **10**(1988), 44-55
11) Ikeuchi, K. : IEEE Trans. Pattern Anal. & Mach. Intell., **3**(1981), 661-669
12) Nishino, E. and Shirai, Y. : The Special Interest Group Notes OF IPSJ, NO.031-002(1984), Inf. Process. Soc. Jpn.
13) Nishimura, T., Fujimura, S., Ito, N. and Kiyasu, S. : Trans. IEE Jpn., **112**-C(1992), 97-101
14) Yamada, K. and Nakano, M. and Yamamoto, S. : Trans. IEE Jpn., **115**-C(1995), 396-402
15) Liu, C. Y., Li, J., Vandentop, G. J., Choi, W. J. and TU, K. N. : J. Electron. Mater., **30**(2001), 521-525
16) Yang, W., Jr. Messler, R. W. and Felton, L. E. : J. Electron. Mater., **23**(1994), 765-772
17) Japanese Standards Association : JIS Z 3197, (1999) Japanese Standards Association, Tokyo
18) Wassink, R. J. K. : Soldering in Electronics, Trans. by Takemoto, T. and Fujiuchi, S., (in Japanese), (1986), 49, The Nikkan Kogyo Shinbun, LTD., Tokyo

(Report received on May 20, 2004)

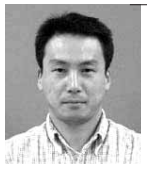

Hisaaki Takao
Year of birth : 1967
Division : Inorganic Materials Lab.
Research fields : Inorganic materials, Microelectronics technology
Academic degree : Dr. Eng.
Academic society : Jpn. Inst. Met., Jpn. Inst. Electron. Packaging
Awards : Paper Awards, MATE, 1999
R&D 100 Awards, 2003

Toshihiko Tsukada
Year of birth : 1963
Division : Robotics Lab.
Research fields : Development and application of image sensing technology
Academic degree : Dr. Eng.
Academic society : Inst. Electr. Eng. Jpn., Inst. Electron. Inf. Commun. Eng.
Awards : R&D 100 Awards, 2003

Keiichi Yamada
Year of birth : 1961
Division : Human Error Prevention Lab.
Research fields : Machine vision, Human factors
Academic degree : Dr. Eng.
Academic society : IEEE, Inst. Electron. Inf. Commun. Eng.
Awards : R&D 100 Awards, 2003

Masahiko Yamashita
Year of birth : 1972
Division : Mechano-electronic Technology Sec.
(Engineer ; Development of measurement system)
Awards : R&D 100 Awards, 2003

Hideo Hasegawa
Year of birth : 1942
Division : Metallic Materials Lab.
Research fields : Metals and Inorganic materials, Microelectronics technology
Academic degree : Dr. Eng.
Academic society : Jpn. Inst. Met., Ceram. Soc. Jpn.
Awards : Paper Awards, The Japan Inst. of Metals, 1987
Paper Awards, MATE, 1999
R&D 100 Awards, 2003